




Research Article

Grain characteristics, electrical conductivity, and hardness of Zn-doped Cu–3Si alloys system

K. C. Nnakwo¹  · F. O. Osakwe¹ · B. C. Ugwuanyi² · P. A. Oghenekowho³ · I. U. Okeke¹ · E. A. Maduka⁴

Received: 10 April 2021 / Accepted: 29 August 2021

Published online: 04 October 2021

© The Author(s) 2021 [OPEN](#)

Abstract

The grain characteristics, electrical conductivity, hardness, and bulk density of Cu–3Si–(0.1–1 wt%)Zn alloys system fabricated by gravity casting technique were investigated experimentally using optical microscopy (OM), scanning electron microscopy (SEM), and energy dispersive spectroscopy (EDS). The study established the optimal alloy composition and the significance of zinc addition on the tested properties using response surface optimal design (RSOD). The cooled alloy samples underwent normalizing heat treatment at 900 °C for 0.5 h. The average grains size and grains distribution were analyzed using the linear intercept method (ImageJ). The microstructure examination revealed a change in grain characteristics (morphology and size) of the parent alloy by addition of 0.1 wt% zinc. The average grains size of the parent alloy decreased from 12 μm to 7.0 μm after 0.1 wt% zinc addition. This change in grain characteristics led to an increase in the hardness of the parent alloy by 42.2%, after adding 0.1 wt% zinc. The electrical conductivity of the parent alloy decreased from 46.3%IACS to 45.3%IACS, while the density was increased by 8.4% after adding 0.1 wt% zinc. The statistical data confirmed the significance of the change in properties. The result of optimization revealed Cu–3Si–0.233Zn as the optimal alloy composition with optimal properties. The Cu–3Si–xZn alloy demonstrated excellent properties suitable for the fabrication of electrical and automobile components.

Keywords Copper-based alloys · Grain characteristics · Hardness · Electrical conductivity · Bulk density

1 Introduction

The superconductivity, ductility, and malleability of copper guarantee its choice over other non-ferrous materials for the fabrication of electrical devices and building components. Copper–silicon alloy system is known to be promising materials for windings for high pulse magnet, integrated circuit lead frames, micro-electronics devices, electrical connectors, accelerators, divertors, and Li-ion batteries, etc. [1, 2]. It has also been proven to be a good catalyst for production of nanosized and nanotube zinc

oxide rod [2–9]. The solubility range of silicon in a copper matrix and vice versa have been studied [10]. The crystal structure and the stability of possible phases in Cu–Si alloy system have also been investigated at different temperature and cooling rates [11]. It was established that Cu–Si alloy system forms Cu₃Si, Cu₁₅Si₄, and Cu₅Si as the major second phases at different Cu/Si ratio, temperature, and cooling rate. The excellent ductility and malleability of copper-based alloys have made it a choice for the fabrication of bolts, nuts, valves, and fittings [3]. Copper gains high strength with much reduction of its

✉ K. C. Nnakwo, kc.nnakwo@unizik.edu.ng | ¹Department of Metallurgical and Materials Engineering, Nnamdi Azikiwe University, Awka, Nigeria. ²Department of Metallurgical and Materials Engineering, Enugu State University of Science and Technology, Agbani, Nigeria. ³Department of Mechanical Engineering, Federal University of Petroleum Resources, Effurun, Nigeria. ⁴Department of Materials Science and Engineering, African University of Science and Technology, Abuja, Nigeria.



electrical conductivity through the process of alloying, work hardening, and subsequent aging treatment [2–12]. The strengthening mechanism of copper-based alloys involves precipitation of hard phases, depending on the alloy compositions. Studies [13, 14] revealed that the addition of silicon to copper melt induced the precipitation of hard phases: Cu_3Si (η_1), $\text{Cu}_{15}\text{Si}_4$ (ϵ), and Cu_5Si (γ). Nickel improves the strength and electrical conductivity of copper–silicon alloys after aging heat treatment, through the inducement of precipitation of intermetallic phases such as $\beta_1\text{-Ni}_3\text{Si} + \alpha\text{-Cu}(\text{Ni}, \text{Si})$, $\gamma'\text{-Ni}_3\text{Al}$, $\beta\text{-Ni}_3\text{Si}$, and $\delta\text{-Ni}_2\text{Si}$ [7–12, 15, 16]. Tungsten, tin, magnesium, manganese, chromium, iron, zirconium, and aluminum enhance the strength and the electrical conductivity of Cu–Ni–Si alloys after aging heat-treated [2–12, 15–24]. Silicon increases the fluidity, hardness, and damping properties of copper-based alloys, hence makes them useful for the fabrication of musical equipment, lithium-ion battery electrode, and catalyst used in zinc oxide rods production [11, 25–29].

Li et al. [19] in their study was able to obtain Cu–8.0Ni–1.8Si–(0.6Sn + 0.15 Mg) alloys with maximum electrical conductivity of 26.5%IACS and hardness of 345 HV through work hardening and subsequent aging heat treatment. Huang et al. [30] replaced Sn and Mg with Zn in the Cu–Ni–Si alloys and recorded an increase in electrical conductivity (from 26.5%IACS to 31%IACS). Eungyeong et al. [23] achieved a further increase in electrical conductivity (from 31%IACS to 43%IACS) via reduction of the nickel content (from 8 wt% to 3wt%), doping with titanium and subsequent aging. Božić et al. [31] achieved increased hardness and electrical conductivity of the Cu–Ni–Si–Ti alloys through the dispersion of TiSi_2 -phase in the copper matrix. Lei et al. [20] developed copper–nickel–silicon–aluminum alloys of excellent hardness (343 HV) and low electrical conductivity (28.1%IACS). The combined addition of phosphorus and magnesium has proved effective in improving the electrical conductivity of Cu–1.5Ni–0.3Si alloys [24]. Puathawee et al. [32] recorded an average hardness of 123.4 HV for Cu–2Si alloy via the addition of 39.5wt% Zn. Li et al. [16] and Wang et al. [22] developed Cu–Ni–Si–Cr–Zr alloys of average hardness (197 HV) and electrical conductivity (32.7%IACS). Xiao et al. [33] in their study increased the electrical conductivity of the Cu–Ni–Si alloys from 32.7%IACS to 47%IACS through single addition of zirconium and subsequent thermomechanical treatment. A combined effect of 0.5wt%Al + 0.15wt%Mg + 0.1wt%Cr in Cu–6.0Ni–1.0Si alloys yielded lower electrical conductivity (25.2%IACS) compared with the single addition of zirconium through thermomechanical and aging treatments [10]. A study carried out by Yi et al. [34] established that, with the addition of Ag, work hardening, and subsequent aging heat treatment, Cu–2.0Ni–0.5Si alloy recorded

average micro-hardness (203 HV) and electrical conductivity (36.4%IACS).

Researchers have explored different mechanisms for the development of high strength, hardness, and superconductive copper-based alloys, but the achievement of combined excellent properties remains difficult. Cu–Be alloys have been revealed to be superconductive and high strength but showed poisonous characteristics which limit their applications in engineering [35, 36].

In this study, the authors focused on refining and modifying the dendritic structure of Cu–3Si alloys system by the addition of zinc nano-particles, cooling of the alloy samples inside a steel mold, and subsequent normalizing heat treatment (at 900 °C for 0.5 h). The grain characteristics (morphology, size, and distribution) were analyzed. The experimental data were analyzed statistically using RSOD to establish the significance of zinc addition on the measured properties, the optimal alloy composition, and generate model equations for subsequent applications.

2 Experimental procedure

The analytical grades copper wire, silicon powder (1–2 μm), and zinc nano-powder (40–60 nm) utilized for this experimental study were supplied by Sigma-Aldrich with % purity of 99.99, 99.8, and 99.99, respectively. The alloys compositions were designed using response surface optimal design (RSOD) and the melting performed in a platinum crucible under inert gas atmosphere. During the melting process, for each alloy composition, about 2 kg of copper was charged into a preheated platinum crucible (at 200 °C). The temperature of the platinum crucible was gradually increased until the copper melted at 1084 °C. The copper melt was superheated to 1100 °C to increase its fluidity. The required amounts of silicon and zinc powder were introduced into the copper melt while wrapped in an aluminum foil to avoid agglomeration and loss of the elements. The mixture was maintained at that temperature for 2 min and stirred vigorously for complete homogeneity. The mixture was cast in a preheated permanent steel mold (at 200 °C) with internal dimensions of 250 mm by 16 mm and cooled slowly to room temperature inside the steel mold.

With the aid of a tube furnace (TSH12/25024166CG) with inbuilt external thermocouple (± 1 °C accuracy), the alloys samples underwent a normalizing heat treatment process at 900 °C for 0.5 h. The samples were ground using a silicon carbide paper of 400 μm grit size to remove the oxide layer after the heat treatment process. For the Vickers hardness test, three indentations were made on each of the sample surface after been ground and polished with the aid of an electric grinder and aluminum oxide

powder, respectively. With the aid of a Vickers hardness tester (Model: VM-50), the indentations were made applying a load of 183.9kgf at 5 s dwell time and the diagonals of indentations measured using a 20X Olympus BH optical microscope. The average diameter of indentations was obtained and the Vickers hardness calculated using Eq. 1. The electrical conductivity of the developed samples was measured using Standard ohms experiment and converted into International Annealed Copper Standard (IACS) using Eq. 2. The bulk density of the developed alloys was calculated applying Archimedes principle (Eq. 3).

With the aid of L2003A type optical microscope (OM) and Carl Zeiss SEM (EVO/NA10), the surface morphology of the developed alloys samples was analyzed. The elemental composition of the developed alloys system was analyzed using EDS. Prior to the analyses, the samples surfaces were ground and polished using silicon carbide papers (400, 800, 1000, and 1200 μ grit sizes) and aluminum oxide powder, respectively. The samples were etched in 8 g FeCl_3 + 20 ml HCl + 120 cm^3 H_2O for 30 s and dried using hot air gun machine (Bosch PHG500-2-1600 W). The grain size distribution was analyzed using linear intercept method (ImageJ software) and the average grain size determined using Eq. 4.

$$\text{HV} = 1.8544 \cdot \frac{P}{d^2} \quad (1)$$

where HV = Vickers hardness (HV).

P = applied load (kgf).

d = average length of diagonals of indentations (μm).

$$\text{Electrical conductivity (\%IACS)} = \frac{172.41}{\text{Resistivity } (\Omega\text{m})} \quad (2)$$

$$\rho = \frac{\rho_{w(T)} W_a}{W_a - W_w} \quad (3)$$

where ρ = bulk density (kg/m^3).

W_a = weight of the sample in air (g).

W_w = weight of the sample in water (g)

$\rho_{w(T)}$ = density of water ($10^3 \text{ kg}/\text{m}^3$).

$$\text{Average grain size} = \frac{\text{Line Length}}{\text{Number of Grains}} \quad (4)$$

2.1 Response surface optimal design

Response surface optimal design (RSOD) is a statistical tool for engineering materials design and optimization of processing techniques and other factors necessary for the improvement of materials properties at minimum cost [38]. RSOD helps researchers to establish the significant

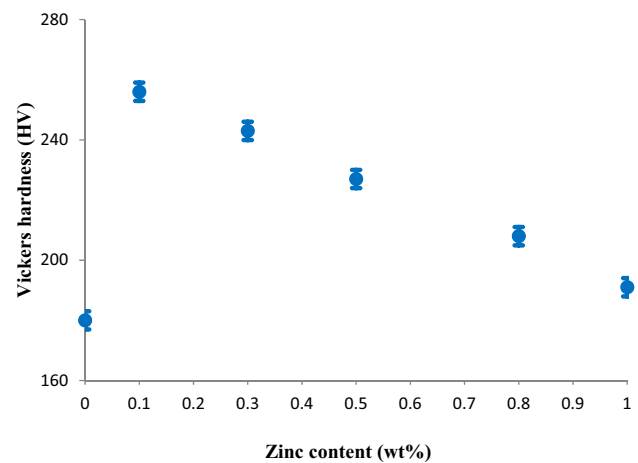


Fig. 1 Hardness of silicon bronze with varying zinc nano-particles content

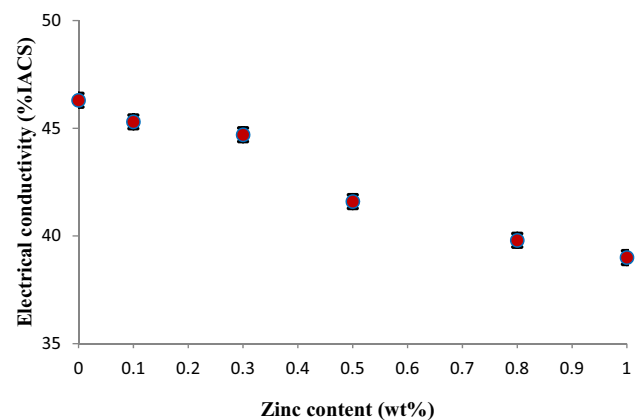


Fig. 2 Electrical conductivity of silicon bronze with varying zinc nano-particles content

effect of processing methods and their interactions on the properties of engineering materials. In this study, the authors adopted RSOD for designing the alloy compositions, determining the significant effect of zinc nano-particles on the measured properties, and establish the optimal alloy composition and model equations for subsequent studies on the said alloys.

3 Results and discussion

3.1 Hardness, density, and electrical conductivity of the developed alloys

Figures 1, 2, and 3 show the variations of hardness, electrical conductivity, and bulk density of parent alloy (Cu–3Si) with concentrations of zinc. The experimental results revealed the hardness, electrical conductivity, and bulk

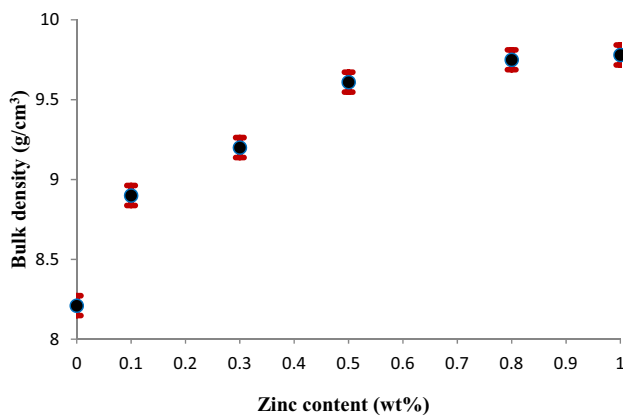


Fig. 3 Bulk density of silicon bronze with varying zinc nano-particles content

density of the parent alloy to be 180 HV, 46.3%IACS, and 8.21 g/cm³. The hardness of the parent alloy increased by 42.2% after a trace (0.1 wt%) addition of zinc. The increase in hardness is confirmed to be significant from the statistical data (Table 1). The addition of zinc nano-particles refined and modified the grains of the parent alloy, leading to an improvement of hardness [2, 3, 5, 37]. The improvement of hardness can also be linked with the decrease in the average grains size of the parent alloy from 12 to 7.0 μm by the addition of 0.1 wt% zinc nano-particles (Figs. 1 and 6). The experimental results showed that the hardness of Cu–3Si–xZn alloy decreased with an increasing concentration of zinc, resulting from an increase in grain size from 7.0 to 9.7 μm and increased solid solution region (α-phase, solid solution of zinc in copper) as the zinc content increased from 0.1 to 1 wt%. Figures 2 and 3 showed that the electrical conductivity of the parent alloy decreased from 46.3%IACS to 45.3%IACS after adding 0.1 wt% zinc nano-particle. The electrical conductivity showed a decreasing trend with increasing zinc content. The electrical behavior of the alloys can be attributed to the reduction of free copper atoms in the alloy structure,

resulting from the increasing solubility of zinc in the copper matrix [2, 3, 5, 8, 37]. The density of the parent alloy was increased by 8.4% (from 8.21 g/cm³ to 8.9 g/cm³) after adding 0.1 wt% zinc (Fig. 3). The density of Cu–3Si–xZn alloy increased with an increasing concentration of zinc in the alloy composition.

3.2 Microstructural evolution, grain size distribution and average grain size

Figures 4 and 5 depict the OM and SEM microstructures of the parent alloy and zinc-doped Cu–3Si alloys system with their corresponding EDS. Figure 6 shows the grains size distribution in the Cu–3Si and Cu–3Si–xZn alloys system. The microstructures of the parent alloy presented in Figs. 4a and 5a revealed needle-like or dendritic grains (appearing dark and light green), with an average grains size of 12 μm. The phase (dark) is surrounded by another phase (light green). The morphology of the secondary phases in the parent alloy (Cu–3Si) changed from needle-like structure to spherical patterns (Figs. 4b–d and 5b–e). This indicates complete wettability of grains which led to increase in hardness. It is also observed that the number or distribution of the dark phase decreased with increasing concentration of zinc in the parent alloy system (Cu–3Si), indicating solubility of elements in the copper matrix. The grain size calculation showed that the grain size of the parent alloy decreased from 12 μm to 7.0 μm after been doped with 0.1 wt% zinc. At increasing concentrations of zinc in the Cu–3Si alloy system, an increase in grain size was observed with an increased solid solution region (Figs. 4 and 5), leading to a systematic decrease in hardness. The grain size increased further from 7.0 μm to 9.7 μm at increasing concentrations of zinc from 0.1 wt% to 1 wt%, leading to a decrease in hardness. Figure 6 revealed that the alloy containing 0.1 wt% zinc content showed better grain size distribution compared to other alloy compositions. The EDS spectrums of the developed

Table 1 Statistical data of the experimental results

Properties	Source	Sum of sq	F value	P value	R ² (%)
Hardness (HV)	Model	3799.02	6.74	0.0091	66.92
	A-Zinc content	3594.89	19.14	0.0014	
	A ²	529.20	2.82	0.1241	
	A ³	3645.28	19.41	0.0013	
Conductivity (%IACS)	Model	121.13	381.05	<0.0001	98.58
	A-Zinc content	111.19	699.53	<0.0001	
	A ²	13.21	83.13	<0.0001	
	A ³	1.27	72.55	<0.0001	
Density (g/cm ³)	Model	4.20	119.77	<0.0001	95.61
	A-Zinc content	3.10	176.90	<0.0001	
	A ²	1.27	72.55	<0.0001	
	A ³	1.27	72.55	<0.0001	

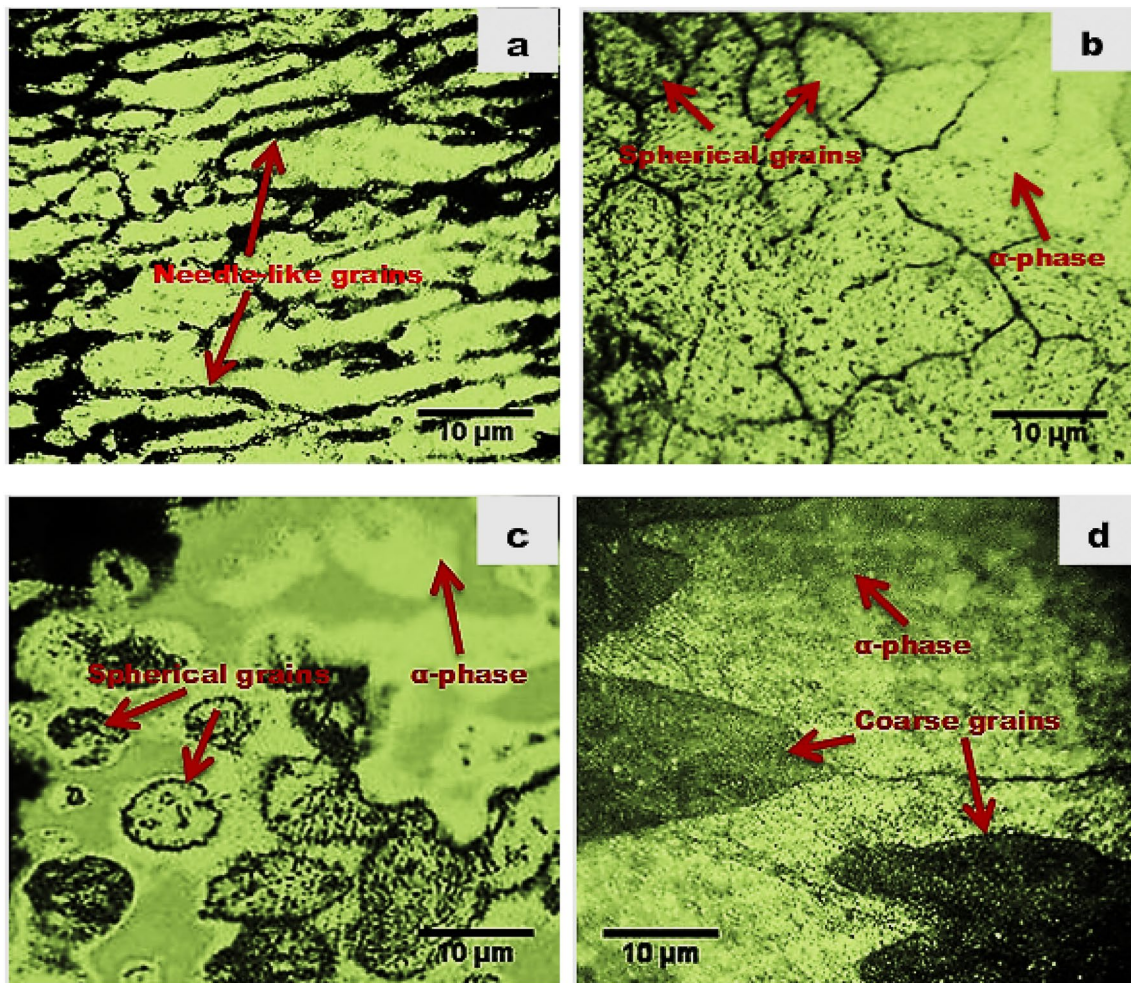


Fig. 4 Optical micrographs of silicon bronzes **a** Cu–3Si, **b** Cu–3Si–0.1Zn, **c** Cu–3Si–0.5Zn, and **d** Cu–3Si–1Zn (Mag: 400x)

alloys system indicate the presence of different elements such as Cu, Si, and Zn.

3.3 Statistical analysis of the experimental results

The experimental results were analyzed statistically to ascertain the significance of the addition of zinc nano-particles on the hardness, electrical conductivity, and bulk density of Cu–3Si alloy. Table 1 shows the results of the analysis. The statistical results showed model F values of 6.74, 121.13, and 4.20 for hardness, electrical conductivity, and bulk density, respectively, indicating significant model terms. From the results, it is shown that the trace addition of zinc nano-particles significantly influenced the hardness, electrical conductivity, and bulk density of the alloy, having recorded *P* values of less than 0.05. The %*R*² values of 66.92%, 98.58%, and 95.61% indicate the likelihood of predicting the significance of zinc nano-particles on the measured properties. The statistical results were optimized and validated using

response surface optimal design (RSOD) to establish the optimal alloy composition for optimal results. The results of optimization as presented in Table 2 showed that the optimal alloy composition, Cu–3Si–0.233Zn gave the optimal results for hardness, electrical conductivity, and bulk density with the desirability of 0.765. This optimization result was validated experimentally. For future applications, the following model equations (Eqs. 5–7) were generated based on the experimental data.

$$\text{Hardness} = +191.80100 + 338.52284\text{Zn} - 603.71465\text{Zn}^2 + 257.27157\text{Zn}^3 \quad (5)$$

$$\text{Electrical conductivity} = +46.52801 + -11.34817\text{Zn} + 3.84326\text{Zn}^2 \quad (6)$$

$$\text{Bulk density} = +8.37445 + 2.71969\text{Zn} - 1.19177\text{Zn}^2 \quad (7)$$

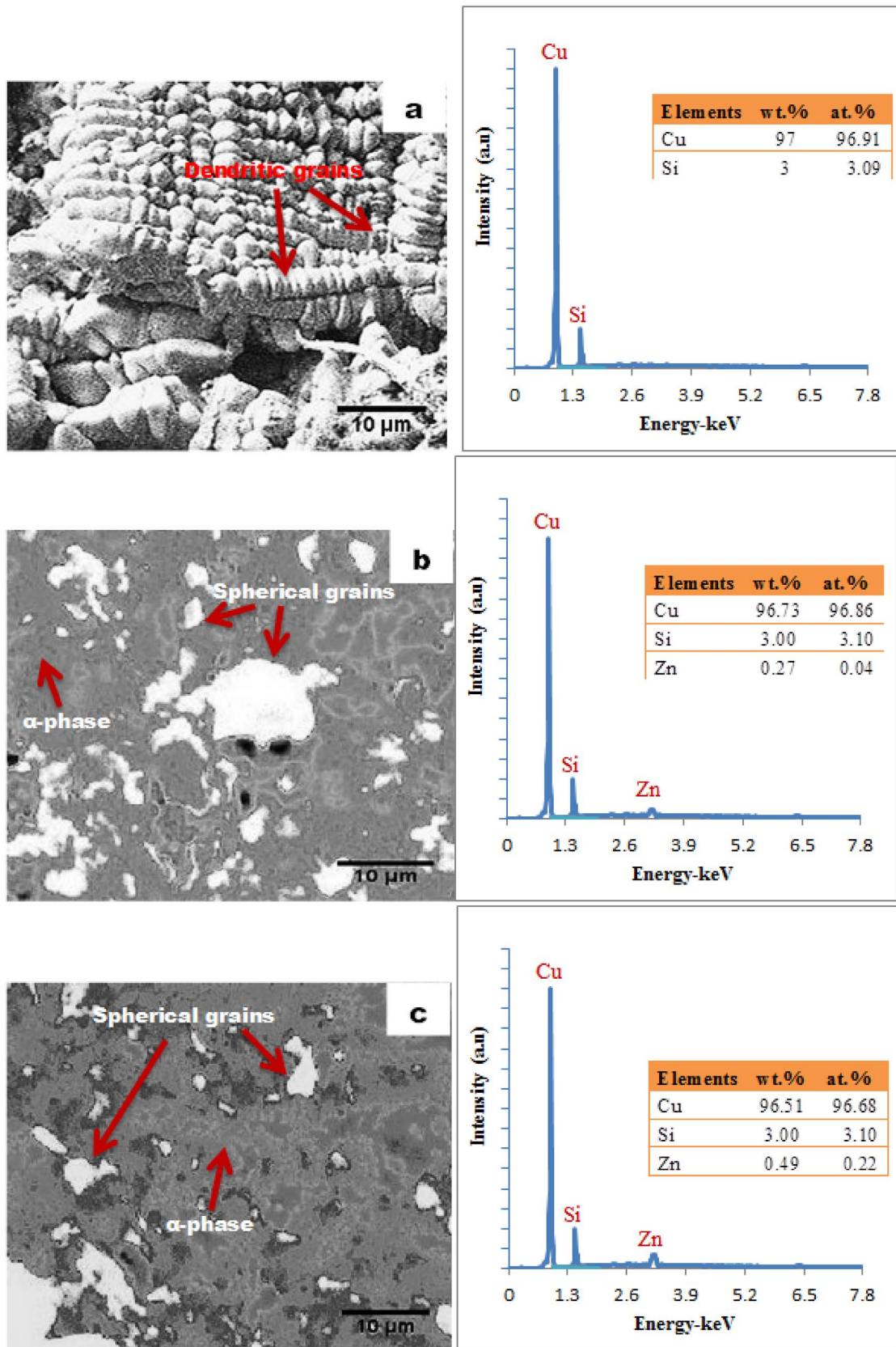


Fig. 5 SEM microstructure of silicon bronzes **a** Cu-3Si, **b** Cu-3Si-0.1Zn, **c** Cu-3Si-0.5Zn, **d** Cu-3Si-0.8Zn, and **e** Cu-3Si-1Zn and their corresponding EDS spectrum (Mag: 3.0kx)

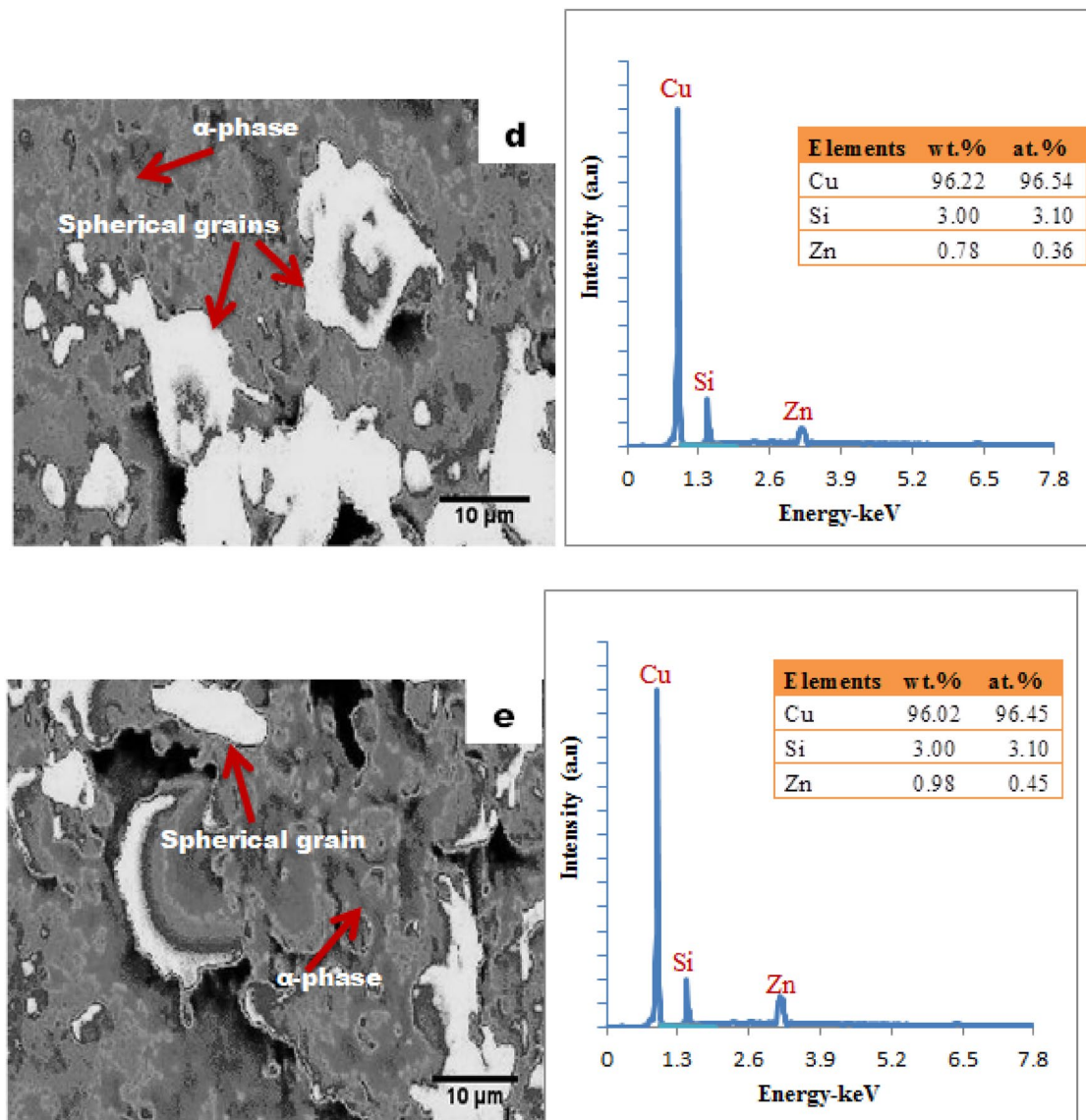


Fig. 5 (continued)

4 Conclusion

The grain characteristics, electrical conductivity, hardness, and bulk density of silicon bronze (Cu–3Si alloy) doped with zinc nano-particles have been investigated experimentally, the optimal alloy composition, and the significance of zinc addition on the studied alloys properties established using RSOD. From the experimental and statistical results, the following conclusions are highlighted:

a. The hardness, electrical conductivity, and bulk density of the parent alloy are 180 HV, 46.3%IACS, and 8.21 g/cm³, respectively.

b. Addition of 0.1 wt% zinc into the parent alloy (Cu–3Si) changed the grain morphology from needle-like to nodular pattern and decreased the grain size from 12 μm to 7.0 μm, leading to about 42.2% increase in hardness.

c. At an increasing concentration of zinc, the grain size increased with a corresponding increase in solid solution region, leading to a decrease in the hardness of Cu–3Si–xZn alloy.

d. The electrical conductivity of the parent alloy decreased by adding 0.1 wt% zinc nano-particle. This electrical behavior could be attributed to the reduction of free copper atoms in the alloy structure, resulting from the increasing solubility of zinc in the copper matrix.

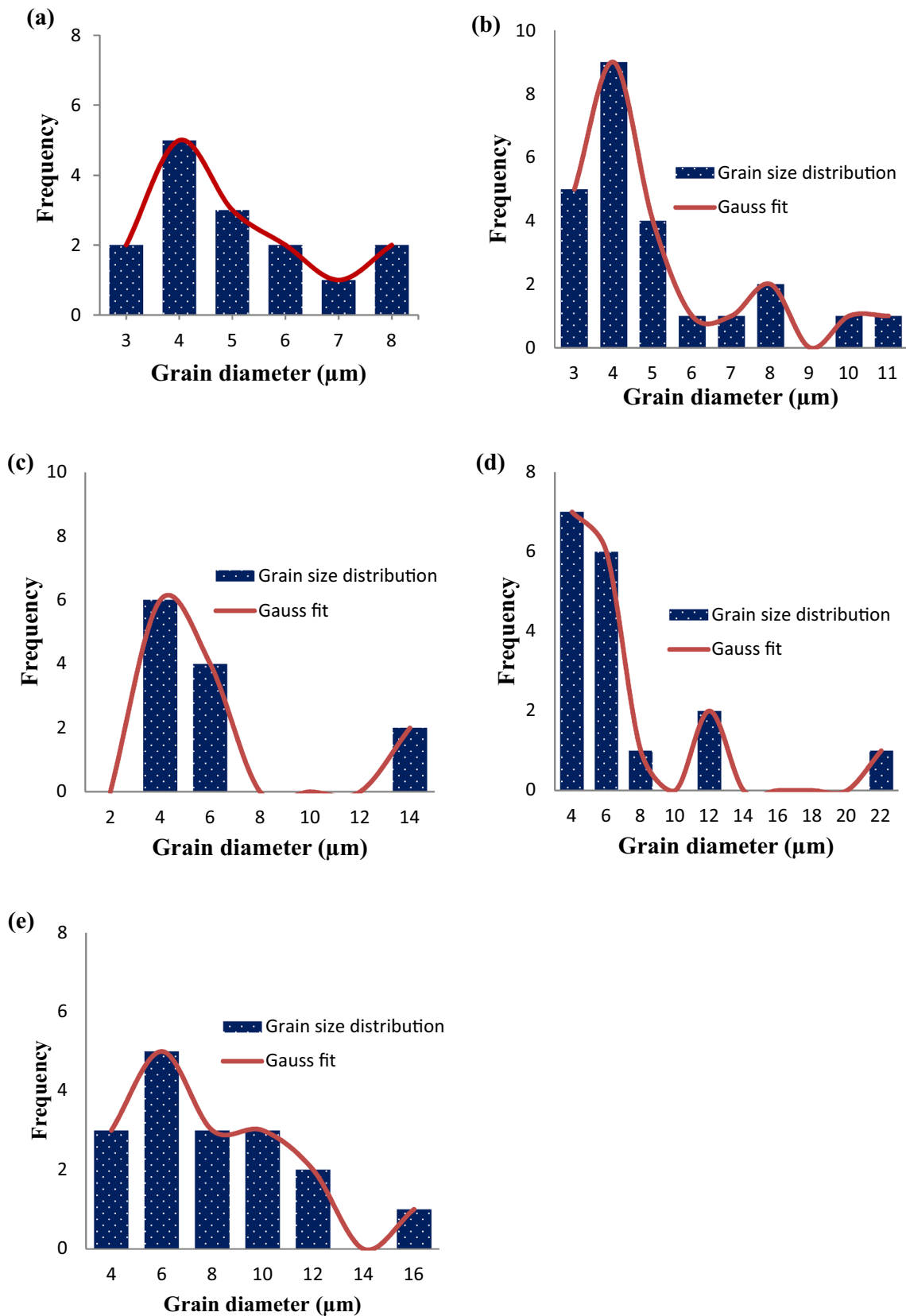


Fig. 6 Grain size distribution in silicon bronzes **a** Cu-3Si, **b** Cu-3Si-0.1Zn, **c** Cu-3Si-0.5Zn, **d** Cu-3Si-0.8Zn, and **e** Cu-3Si-1Zn

Table 2 Optimization and validation of experimental data

Number	Zn content (wt%)	Hardness, (HV)	Conductivity (%IACS)	Density (g/cm ³)	Desirability	Remark
Optimization	0.233	241.150	44.093	8.943	0.765	Selected
Validation	0.233	240.82	45.31	8.853		

e. The density of the parent alloy was increased by 8.4% (from 8.21 g/cm³ to 8.9 g/cm³) after adding 0.1 wt% zinc. The density of Cu–3Si–xZn alloy increased with an increasing concentration of zinc in the alloy composition.

f. The Cu–3Si–xZn alloy containing 0.1 wt% zinc content showed better grain size distribution compared to other alloy compositions.

g. A trace addition of zinc nano-particles into silicon bronze significantly influenced the hardness, electrical conductivity, and bulk density of the alloy, having recorded *P* values less than 0.05 with %*R*² values of 66.92%, 98.58%, and 95.61%, respectively.

h. The optimal alloy composition was Cu–3Si–0.233Zn, having recorded the optimal results for hardness, electrical conductivity, and bulk density with the desirability of 0.765.

Acknowledgements The authors heartily appreciate Engr. Dr. Kingsley C. Nnakwo for his technical support for this study.

Declaration

Conflict of interests The authors declared no conflict of interests.

Open Access This article is licensed under a Creative Commons Attribution 4.0 International License, which permits use, sharing, adaptation, distribution and reproduction in any medium or format, as long as you give appropriate credit to the original author(s) and the source, provide a link to the Creative Commons licence, and indicate if changes were made. The images or other third party material in this article are included in the article's Creative Commons licence, unless indicated otherwise in a credit line to the material. If material is not included in the article's Creative Commons licence and your intended use is not permitted by statutory regulation or exceeds the permitted use, you will need to obtain permission directly from the copyright holder. To view a copy of this licence, visit <http://creativecommons.org/licenses/by/4.0/>.

References

- Jung SJ, O'Kelly CJ, Boland JJ (2015) Position controlled growth of single crystal Cu₃Si nanostructures. *Cryst Growth Des* 15:5355–5359. <https://doi.org/10.1021/acs.cgd.5b00947>
- Nnakwo KC, Okeke IU, Nnuka EE (2017) Structural modification and mechanical properties of Cu–3wt%Si–xwt%Sn alloy. *Int J Sci Res Sci Eng Technol* 3:184–187
- Nnakwo KC (2019) Effect of tungsten content on the structure, physical and mechanical properties of silicon bronze (Cu–3wt%Si). *J King Saud Univ Sci* 31(4):844–848. <https://doi.org/10.1016/j.jksus.2017.12.002>
- Nnakwo KC, Mbah CN, Daniel-Mkpume CC (2019) Investigation of the structural sensitive behavior of Cu–3Si–xMn ternary alloys. *J King Saud Univ Sci* 31:1056–1063. <https://doi.org/10.1016/j.jksus.2019.01.001>
- Nnakwo KC, Mbah CN, Ude SN (2019) Influence of chemical composition on the conductivity and on some mechanical properties of Mg-doped Cu–Si alloy. *J King Saud Univ Eng Sci*. <https://doi.org/10.1016/j.jksues.2019.03.005>
- Nnakwo KC, Nnuka EE (2018) Correlation of the structure, mechanical and physical properties of Cu3wt%Si–xwt%Sn silicon bronze. *J Eng Appl Sci* 13:83–91
- Xie SS, Li YL, Zhu L (2003) Progress of study on lead frame copper alloy and its implementation in electronic industry. *Rare Met* 27:76–79
- Lei Q, Xiao Z, Hu W, Derby B, Li Z (2017) Phase transformation behaviors and properties of a high strength Cu–Ni–Si alloy. *Mater Sci Eng A* 697:37–47. <https://doi.org/10.1016/j.msea.2017.05.001>
- Gholami M, Vasely J, Altenberger I, Kuhn HA, Wollmann M, Janecek M, Wagner L (2017) Effect of microstructure on mechanical properties of CuNiSi alloys. *J Alloys Compd* 696:201–212. <https://doi.org/10.1016/j.jallcom.2016.11.233>
- Qian L, Zhou L, Zhou L, Yang G, Xi P, Benjamin D (2017) Microstructure and mechanical properties of a high strength Cu–Ni–Si alloy treated by combined aging processes. *J Alloys Compd* 695:2413–2423. <https://doi.org/10.1016/j.jallcom.2016.11.137>
- Suzuki S, Shibutani N, Mimura K, Isshiki M, Waseda Y (2006) Improvement in strength and electrical conductivity of Cu–Ni–Si alloys by aging and cold rolling. *J Alloys Compd* 417(1–2):116–120. <https://doi.org/10.1016/j.jallcom.2005.09.037>
- Wang W, Kang H, Chen Z, Chen Z, Li R, Yin G, Wang Y (2016) Effects of Cr and Zr addition on microstructure and properties of Cu–Ni–Si alloys. *Mater Sci Eng, A* 673:378–390. <https://doi.org/10.1016/j.msea.2016.07.021>
- Pak AY, Shatrova KN, Aktaev NE, Ivashutenko AS (2016) Preparation of ultrafine Cu₃Si in high-current pulsed arc discharge. *Nanotechnol Russ* 11(9–10):548–552. <https://doi.org/10.1134/S199507801605013X>
- Mattern N, Seyrich R, Wilde L, Baetz C, Knapp M, Acker J (2007) Phase formation of rapidly quenched Cu–Si alloys. *J Alloys Compd* 429:211–215. <https://doi.org/10.1016/j.jallcom.2006.04.046>
- Qing L, Li Z, Wang MP (2011) Phase transformation behavior in Cu–8.0Ni–1.8Si alloy. *J Alloys Compd* 509(8):361–367. <https://doi.org/10.1016/j.jallcom.2010.12.115>
- Li D, Wang Q, Jiang B, Li X, Zhou W, Dong C, Wang H, Chen Q (2017) Minor-alloyed Cu–Ni–Si alloys with high hardness and electric conductivity designed by a cluster formula approach. *Progress Nat Sci Mater Int* 27(4):467–473. <https://doi.org/10.1016/j.pnsc.2017.06.006>
- Garbacz-Klempka A, Kozana J, Piękoś M, Papaj M, Papaj P, Perek-Nowak M (2018) Influence of modification in centrifugal casting on microstructure and mechanical properties of silicon bronzes. *Arch Foundry Eng* 18:11–18. <https://doi.org/10.24425/123594>
- Pan ZY, Wang MP, Li Z (2007) Effect of trace elements on properties of Cu–Ni–Si alloy. *Mater Rev* 21(5):86–89

19. Li Z, Pan ZY, Zhao YY, Xiao Z, Wang MP (2009) Microstructure and properties of high-conductivity, super-high-strength Cu–8.0Ni–1.8Si–0.6Sn–0.15Mg alloy. *J Mater Res* 24(6):2123–2129. <https://doi.org/10.1557/jmr.2009.0251>
20. Lei Q, Li Z, Dai C, Wang J, Chen X, Xie JM, Yang WW, Chen DL (2013) Effect of aluminium on microstructure and property of Cu–Ni–Si alloys. *Mater Sci Eng A* 572:65–74. <https://doi.org/10.1016/j.msea.2013.02.024>
21. Lei Q, Li Z, Xiao T, Pang Y, Xiang QZ, Qiu WT, Xiao Z (2013) A new ultrahigh strength Cu–Ni–Si alloy. *Intermetallics* 42:77–84. <https://doi.org/10.1016/j.intermet.2013.05.013>
22. Wang W, Guo E, Chen Z, Kang H, Chen Z, Zou C, Lia R, Yina G, Wang T (2018) Correlation between microstructures and mechanical properties of cryorolled CuNiSi alloys with Cr and Zr alloying. *Mater Charact* 144:532–546. <https://doi.org/10.1016/j.matchar.2018.08.003>
23. Eungyeong L, Seungzeon H, Kwangjun E, Sunghwan L, Sangshik K (2011) Effect of Ti addition on tensile properties of Cu–Ni–Si alloys. *Met Mater Int* 17(4):569–576. <https://doi.org/10.1007/s12540-011-0807-7>
24. Ho JR, Hyung KB, Soon HH (2000) Effect of thermo-mechanical treatments on microstructure and properties of Cu-base lead frame alloy. *J Mater Sci* 35(14):3641–3646. <https://doi.org/10.1023/A:1004830000742>
25. Ketut GSI, Soekrisno R, Suyitno MIM (2011) Mechanical and damping properties of silicon bronze alloys for music applications. *Int J Eng Tech IJETJENS* 11(06):81–85
26. Polat BD, Eryilmaz OL, Keleş O, Erdemir A, Amine K (2015) Compositionally graded SiCu thin film anode by magnetron sputtering for lithium ion battery. *Thin Solid Films* 596:190–197. <https://doi.org/10.1016/j.tsf.2015.09.085>
27. Xu K, He Y, Ben L, Li H, Huang H (2015) Enhanced electrochemical performance of Si–Cu–Ti thin films by surface covered with Cu₃Si nanowires. *J Power Sources* 281:455–460. <https://doi.org/10.1016/j.jpowsour.2015.02.023>
28. Moon T, Kim C, Park B (2006) Electrochemical performance of amorphous-silicon thin films for lithium rechargeable batteries. *J Power Sources* 155:391–394. <https://doi.org/10.1016/j.jpowsour.2005.05.012>
29. Cai H, Tong D, Wang Y, Song X, Ding B (2011) Reactive synthesis of porous Cu₃Si compound. *J Alloys Compd* 509:1672–1676. <https://doi.org/10.1016/j.jallcom.2010.09.116>
30. Huang F, Jusheng M, Honglong N, YuWen C, Zhiting G (2003) Precipitation in Cu–Ni–Si–Zn Alloy for lead frame. *Mater Lett* 57:2135–2139
31. Božić D, Dimčić O, Dimčić B, Cvijović I, Rajković V (2008) The combination of precipitation and dispersion hardening in powder metallurgy produced Cu–Ti–Si alloy. *Mater Charact* 5(9):1122–1126
32. Puathawee S, Rojananan S, Rojananan S (2013) Lead-free Cu-Si-Zn brass with tin addition. *Adv Mater Res* 802:169–173
33. Xiao X, Xiong B, Wang Q, Xie G, Peng L, Huang G (2013) Microstructure and properties of Cu–Ni–Si–Zr alloy after thermomechanical treatments. *Rare Met* 32(2):144–149
34. Yi Z, Ping L, Baohong T, Shu GJ, Yong L (2012) Ageing treatment of Cu–Ni–Si–Ag alloy. *Procedia Eng* 27:1789–1793
35. Tsubakino H, Noza R, Yamamoto A (1993) Precipitation sequence for simultaneous continuous and discontinuous modes in Cu–Be binary alloys. *Mater Sci Technol* 19(4):288
36. Masamichi M, Yoshikiyo O (1988) Effect of B additions on the intragranular and cellular precipitations in a Cu–Be alloy. *Mater Trans JIM* 29(11):903
37. Nnakwo KC, Mbah CN, Nnuka EE (2019) Influence of trace additions of titanium on grain characteristics, conductivity and mechanical properties of copper-silicon-titanium alloys. *Heliyon* 5(10):e02471. <https://doi.org/10.1016/j.heliyon.2019.e02471>
38. Hines WW, Montgomery DC, Goldsman DM, Borrer CM (2003) *Probability and Statistics in Engineering*, 4edn, Wiley, New York

Publisher's Note Springer Nature remains neutral with regard to jurisdictional claims in published maps and institutional affiliations.